Co-published by
Institute of Fluid-Flow Machinery
Polish Academy of Sciences
Committee on Thermodynamics and Combustion
Polish Academy of Sciences

http://www.imp.gda.pl/archives-of-thermodynamics/

Numerical Study on Nozzle Group Atomization Cooling: Effects of Pressure, Tilt Angle and Spacing on Enhanced Heat Transfer

Li Li[a,b,*], Rong Li[a,b], Lei Zhang[a,b]

[a]Hebei Key Laboratory of Man-machine Environmental Thermal Control Technology and Equipment, Xingtai, 054000, China
[b]Hebei Vocational University of Technology and Engineering, Xingtai, 054000, China
*Corresponding author email: lili@xpc.edu.cn

Received: 25.12.2024; revised: 23.04.2025; accepted: 27.05.2025

Abstract

This study investigates the improved heat transfer process of multi-nozzle arrangements through numerical analysis. A discrete phase based numerical model is developed to analyse the secondary atomization and heat transfer characteristics under different conditions. The effects of pressure, spacing and tilt angle of the nozzle group on the atomization cooling performance are evaluated. The results indicate that increasing the pressure can significantly improve the heat transfer capacity. The higher the pressure, the lower the hot wall temperatures and the higher the heat transfer coefficient. The nozzle tilt angle also has a significant impact. The heat transfer performance for a 30° tilt angle is optimal, while for a 15° tilt angle is poor. Increasing the number of nozzles can improve the cooling to a limited extent. In addition, nozzle spacing will affect temperature distribution, thereby achieving optimal cooling at intermediate distances. The results can provide valuable insights for optimizing multi-nozzle configurations of efficient heat transfer in industrial applications.

Keywords: Nozzle atomization; Pressure change; Tilt angle; Nozzle spacing; Heat transfer

Vol. 46(2025), No. 2, 143–152; doi: 10.24425/ather.2025.154913

Cite this manuscript as: Li, L., Li, R., & Zhang, L. (2025). Numerical Study on Nozzle Group Atomization Cooling: Effects of Pressure, Tilt Angle and Spacing on Enhanced Heat Transfer. *Archives of Thermodynamics*, 46(2), 143–152.

1. Introduction

The increasing demand for high-performance cooling solutions in various industrial and technological applications such as power generation, electronics and manufacturing has driven the development and optimization of advanced heat transfer techniques. One of the most promising methods is spray cooling, which involves optimizing the liquid into fine droplets on a hot surface, providing rapid and effective heat dissipation. This technique has achieved significant attention due to its ability for high heat transfer coefficients and low thermal resistance [1–4]. Recent advancements in spray cooling have focused on optimizing various parameters, including droplet size, velocity and distribution, to enhance the overall cooling performance [5–8].

In the context of spray cooling, the configuration of nozzle groups is a critical factor influencing the effectiveness of the process. Pressure, spacing and tilt angle of the nozzles can significantly affect the heat transfer characteristics. For instance, higher pressures typically result in finer droplets and increased momentum, leading to improved heat transfer coefficients [9−11]. The spacing between nozzles is also important, as it affects the uniformity of the spray coverage and the overlap of the atomization cones, which in turn impacts the heat transfer efficiency [12,13]. Furthermore, the tilt angle of nozzles can alter the impingement pattern and the distribution of droplets on the target surface, thereby affecting the heat transfer rate [14]. Understanding these relationships is essential for the design and optimization of efficient spray cooling systems.

Nomenclature

Abbreviations and Acronyms

CHF – critical heat flux
DPM – discrete phase model
PISO – pressure implicit split operator
SMD – Sauter mean diameter
TAB – Taylor analogy breakup

Numerous studies have shown the effects of different nozzle configurations on the heat transfer performance of spray cooling. Durmus et al. [15] examined the heat transfer performance and pressure drop characteristics in concentric heat exchangers of a volute inlet, and analysed the heat transfer efficiency and fluid resistance under different operating conditions. Abbasi and Kim [16] explored the application of nano-fluids in spray cooling, and found that the addition of nanoparticles can significantly enhance the heat transfer coefficient. Combined with a newly designed conical wire blade, Oflaz et al. [17] investigated the thermal properties of SiO_2-water nano-fluid. The study also highlighted the potential of nano-fluids to improve thermal performance. Cheng et al. [18] experimentally and numerically investigated the impact of different nozzle configurations on spray cooling, demonstrating that optimal spacing and inclination angles can improve the cooling efficiency. Wang et al. [19] studied the heat transfer performance of spray cooling under low mass flux conditions and highlighted the importance of droplet size and velocity.

Hou [20] conducted numerical simulations and experimental validations to multi-nozzle spray cooling systems, providing valuable insights into the optimal nozzle arrangements for improved heat transfer. Zhang et al. [12] and Muthukrishnan et al. [21] developed the correlations to predict the critical heat flux (CHF) in spray cooling, which is crucial for the safe and efficient operation of cooling systems. The applications of implementing spray cooling in real-world applications are also concerned. Pautsch and Shedd [8] measured the thickness of liquid film during spray cooling of FC-72, providing data that can be used to optimize the cooling process. Liao et al. [22] developed a comprehensive model to predict the performance of simplex atomizers, which are commonly used in spray cooling systems. Si et al. [23] tested an integrated refrigeration-spray cooling system for high-power solid-state lasers and demonstrated the potential of spray cooling in specialized applications. These studies emphasize the importance of considering theoretical and practical aspects for designing and optimizing spray cooling systems.

Despite the above advancements in spray cooling, a comprehensive understanding of the intricate interactions in different parameters remains to be fully explained. This study aims to develop a gas-liquid two-phase atomization and heat transfer model for a pressure swirl nozzle array, and systematically analyse the influence of nozzle atomization cooling on improved heat transfer performance. This study focuses on different configurations of nozzle groups, simulating atomization and heat transfer processes on heated walls by numerically calculating the droplet ejection at the nozzle outlet and its subsequent trajectory in the computational domain. Based on these simulations, an in-depth examination is conducted considering the effects of pressure, tilt angle and spacing on the atomization characteristics of the nozzle array. These findings can not only provide essential insights for optimizing nozzle atomization cooling parameters, but also provide robust data support for advancing the comprehension of enhanced heat transfer mechanisms. The practical significance lies in its capacity to improve the efficiency and reliability of industrial cooling systems through refining nozzle configurations. This is particularly important in power generation, electronics and manufacturing. Efficient cooling solutions are indispensable in these fields, and can provide scientific foundations and technical guidance.

2. Research method

A numerical model utilizing ANSYS Fluent software based on the discrete phase model (DPM) is developed to investigate the secondary atomization and heat transfer characteristics of multiple nozzles under different operating conditions. The examined parameters include nozzle group pressure, spacing and tilt angle. The DPM model is selected to accurately track individual droplets and predict their interactions with heated surfaces. To ensure the reliability of the model, grid independence is verified. The numerical results are validated with experimental data from previous studies to evaluate the impact of these parameters on atomization cooling performance.

2.1. Verification of grid independence

In this study, pressure swirl nozzles are used for numerical simulation of the atomization characteristics of the nozzle group and for the numerical simulation of cooling. The cooling medium is accelerated by the cyclone sheet, and then enters the central cyclone chamber to form a central air column under centrifugal force. When the cooling medium leaves the nozzle outlet, it is already in the state of liquid film. This is because the surface tension of the liquid film is unstable at this time, and then it decomposes into filamentous liquid or liquid droplets. Due to the fact that the numerical simulation mainly explores the spatial injection of droplets in the nozzle group of the computational domain, as well as the formation of liquid film and the heat transfer on the bottom hot surface, the central region is encrypted and the boundary layer grid is set on the bottom surface when dividing the grid. To further verify the grid independence of this model, the rectangular computational domains with about 50 000, 263 000, 386 000, 483 000 and 781 000 grid cells are used to verify the grid independence, respectively. The DPM condition of the bottom surface is set as escape and the time step is 1×10^{-5} s to run for 2000 steps. The Sauter mean diameter (SMD) of droplets injected by the nozzle is recorded for judgment based on the change in SMD of droplets. The results are shown in Fig. 1.

When the number of grid cells reaches 483 000, SMD of droplets hardly changes with this increase. Therefore, to shorten the calculation time, the calculation model with 483 000 grid cells is adopted to establish the independence of the model grids.

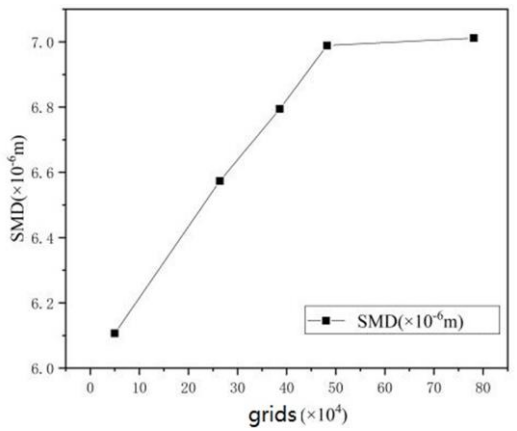

Fig. 1. Mesh independence verification.

2.2. Numerical calculation settings

ANSYS Fluent is used for numerical simulation. The boundary conditions for the continuous phase are established with a pressure inlet, while the flow of the continuous gas phase (air) in the computational domain is induced by liquid droplets ejected from a lateral injection source. The bottom boundary of the computational domain is modelled as an adiabatic wall without slip, maintained at a temperature of 293 K. All other boundaries in the computational domain are designated as pressure outlets. A realizable k–ε turbulence model is adopted. A second-order upwind scheme is used for pressure and momentum calculations via the pressure implicit with splitting of operator (PISO) algorithm.

Under the background of setting discrete phase boundary conditions, a pressure cyclone nozzle is used to precisely define parameters such as the inlet pressure and flow rate. The DPM boundary conditions on the upper surface around the computational domain and at the nozzle location are specified as escape, while those on the bottom surface are configured to trap particles. A random tracking model is used for particle tracking, and a dynamic drag model and a Taylor analogy breakup (TAB) model are used to explain the effect of gravity on droplets.

The inlet temperature of the cooling medium (water) and the ambient temperature are both maintained at 293 K. The material of the bottom heating wall is copper. The thermal wall is configured to be non-slip, with a heat flux set at 100 W/cm². Droplets are tracked as they reach the hot wall surface to form a liquid film. Consequently, the above Eulerian wall film model is activated, and the bottom boundary condition is defined as wall-jet.

2.3. Model reliability verification

To validate the reliability of the heat transfer model for the nozzle group, numerical simulations are conducted using the experimental conditions in Ref. [17]. Figure 7 shows the simulation results of nozzle atomization cooling in a wall temperature range of 40–90℃. As shown in Fig. 2, the discrepancy between the numerical simulations and experimental results remains within 10% in the temperature range of 40–90℃. This deviation may be attributed to the experimental conditions and measurement inaccuracies. The uncertainty related to temperature readings and droplet size distributions can affect the interpretation of results. Although the DPM model is effective for simulating discrete phase flow, its limitations in predicting secondary droplet fragmentation and coalescence under specific conditions should also be considered. Given that the error is in an acceptable range, the used heat transfer model is reliable.

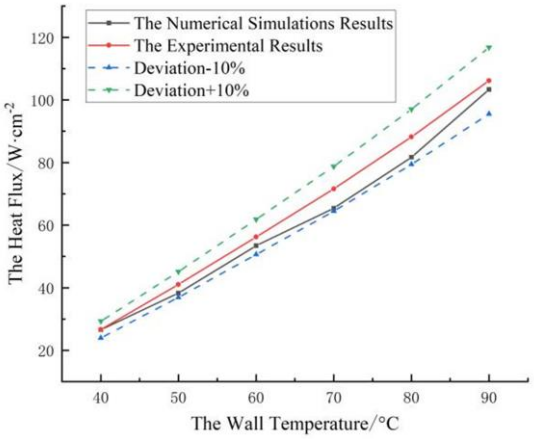

Fig. 2. Comparison between numerical simulations and experimental results of the heat transfer model.

3. Results and discussion

3.1. Effect of different pressures

The heat transfer mechanisms in spray cooling include the direct thermal exchange between the cooling medium and high-velocity liquid droplets impacting on the heating surface via the nozzle, as well as the heat transfer from the liquid film formed by these droplets on the hot surface, the flow of this liquid film over said surface, and its subsequent evaporation. To investigate how pressure influences the heat transfer characteristics of the nozzle array, a constant heat flux of 100 W/cm² is maintained while simulating spray cooling pressures ranging from 1.0 MPa to 2.0 MPa. Figure 3 shows the changes in bottom surface temperature under different pressure conditions.

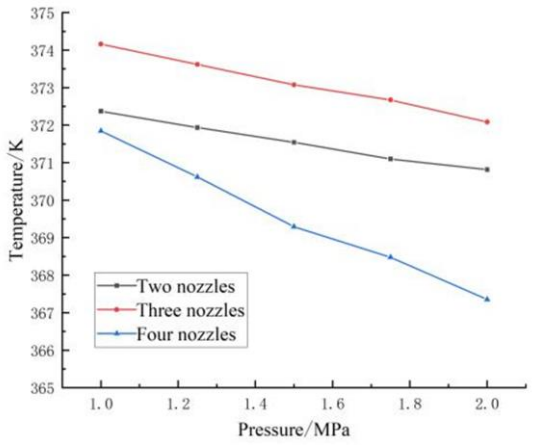

Fig. 3. Temperature curves under different pressure conditions.

The data indicate that the two, three and four nozzles have similar trends. Specifically, as pressure increases, there is a corresponding decrease in average hot wall temperature. This phenomenon can be attributed to the increased atomization effect caused by the increase in pressure, which increases the energy of droplet fragmentation, reduces droplet size, accelerates droplet velocity, and thus enhances their heat transfer ability.

Figures 4, 5 and 6 show the temperature distribution on the bottom surface of the two, three and four nozzles under different pressure conditions. As nozzle pressure increases from 1.0 MPa to 2.0 MPa, the strong impact region and the blue low-temperature zone within the atomization cone both transition from a discontinuous state to a completely continuous state. At the same time, the area occupied by red high-temperature regions associated with weak impacts within the atomization cone gradually decreases. It is worth noting that an extension of this red high-temperature region occurs near the atomization cone. However, it decreases along with the temperature. This phenomenon, which can be attributed to an increase in droplet velocity, will increase the pressure, resulting in a decrease in average droplet diameter while promoting a more uniform distribution of droplets. Therefore, the heat transfer capabilities in the impact areas of the atomizing cone can be enhanced, and the thermal effects related to liquid film flow outside this region can be improved.

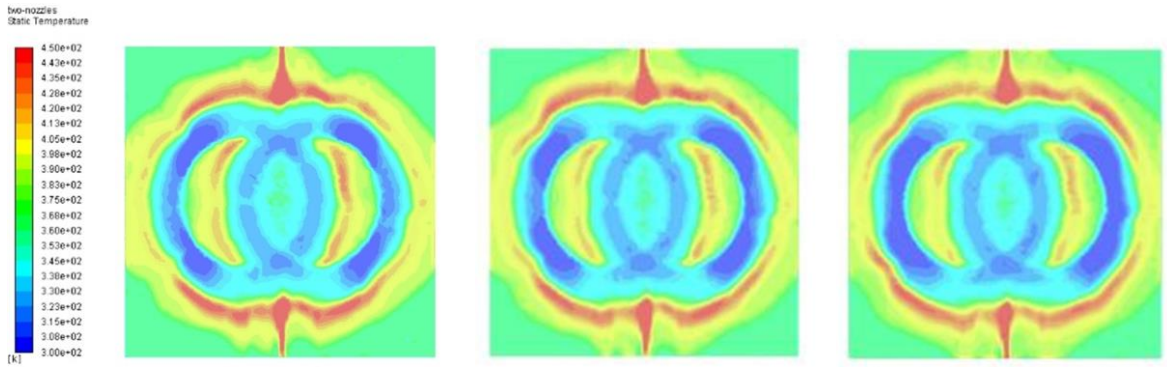

(a) 1.0 MPa (b) 1.5 MPa (c) 2.0 MPa

Fig. 4. Temperature distribution on the bottom surface of two nozzles under different pressures.

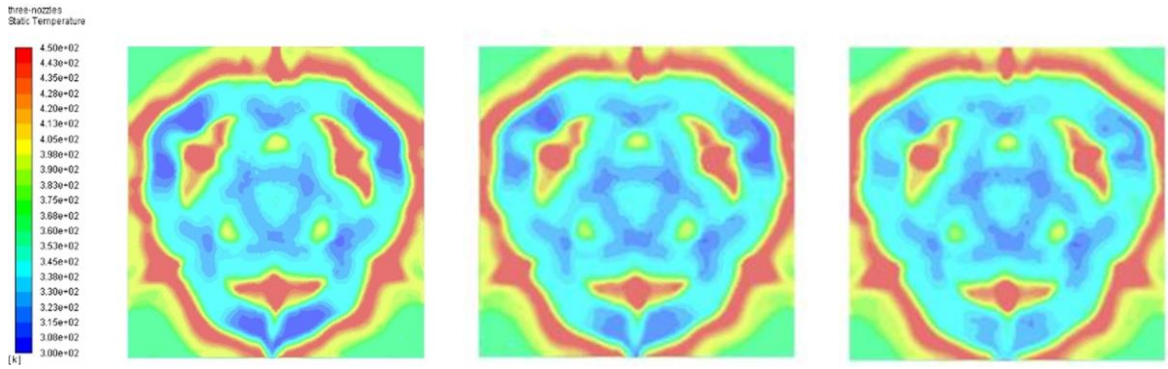

(a) 1.0 MPa (b) 1.5 MPa (c) 2.0 MPa

Fig. 5. Temperature distribution on the bottom surface of three nozzles under different pressures.

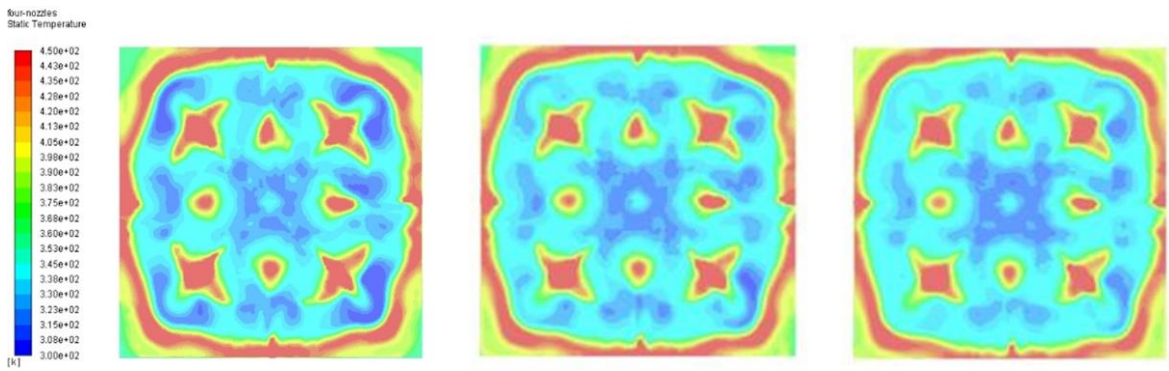

(a) 1.0 MPa (b) 1.5 MPa (c) 2.0 MPa

Fig. 6. Temperature distribution on the bottom surface of four nozzles under different pressures.

Under consistent pressure conditions, an increase in the number of nozzles leads to a gradual expansion of the coverage area of the atomization cone. The blue low-temperature region in the atomization cone extends outward, while the interference zone becomes more dispersed. However, the central blue low-temperature area has a significant increase. The number of red high-temperature regions with weak impact inside the atomization cone increases, showing a clear regularity. On the contrary, the area and temperature of the extrapyramidal region will decrease. This phenomenon can be attributed to the increase in the number of nozzles, which leads to an increase in the atomization region and an expanded interference zone between nozzles, thereby improving the heat transfer area and efficiency.

Figure 7 shows the variation in the hot wall heat transfer coefficient for the two, three and four nozzles under different pressures. The data indicates that as the pressure increases, the heat transfer coefficient of the hot wall also increases. Notably, the range of variation in this coefficient is most significant for four nozzles and least pronounced for two nozzles. The heat transfer coefficients in all three nozzle configurations exceed 15 000 W/(m^2·K). This suggests that increasing the number of nozzles can significantly enhance the heat transfer of the atomizing cooling system on the bottom surface of the nozzle group.

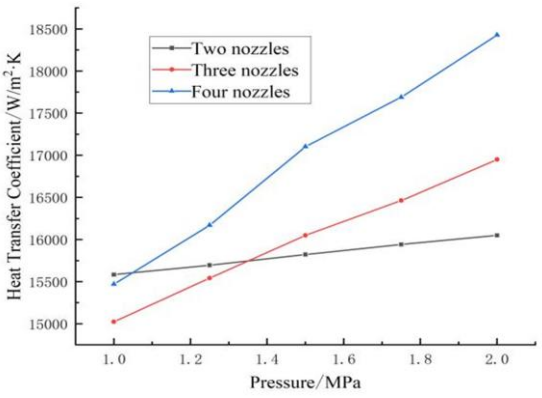

Fig. 7. Heat coefficient curves under different pressure inlet conditions.

According to Figs. 3 through 7, as shown in Table 1 below, the parameters of different nozzle groups change under different pressures: as the pressure increases, the average droplet velocity increases; the bottom surface average temperature decreases, and the bottom heat transfer coefficient increases.

Table 1. Parameters of the nozzle group under different pressures.

Number of nozzles	P, MPa	Average bottom surface temperature, K	Average liquid film temperature, K	Heat transfer coefficient, W/(m²·K)
Two	1.0	372.37	308.19	15582.54
	1.5	371.54	308.33	15821.40
	2.0	370.81	308.50	16049.54
Three	1.0	374.16	307.59	15023.26
	1.5	373.07	310.76	16048.27
	2.0	372.08	313.08	16949.58
Four	1.0	371.84	307.20	15469.86
	1.5	369.29	310.81	17101.45
	2.0	367.35	313.08	18426.51

This indicates that increasing pressure can improve the atomization effect of the nozzle group and its heat transfer capability, which is crucial for designing efficient multi-nozzle array cooling systems.

3.2. Effect of different tilt angles

Figure 8 shows the trend of the average bottom surface temperature of the two, three and four nozzles at different tilt angles. The findings indicate that as the nozzle tilt angle increases, the bottom temperature first increases and then decreases. Notably, the two and three nozzles exhibit a similar trend, reaching a comparable minimum temperature at 30°. The four nozzles display a more pronounced variation in temperature and achieve a similar temperature at both 0° and 30°.

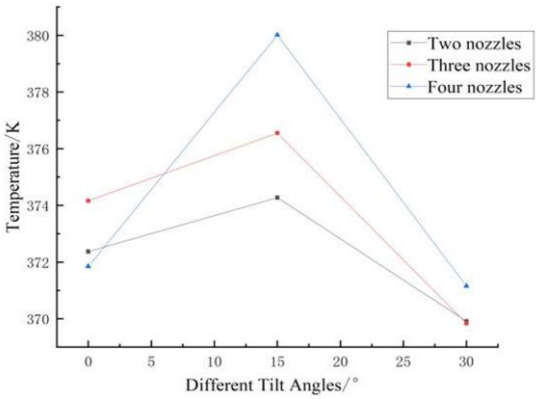

Fig. 8. Temperature curves at different tilt angles.

Based on the temperature distribution of the hot wall in Figs. 9, 10, and 11, it is observed that the coverage area of the atomization cone changes as the tilt angle increases. The temperature in the strong impact region of the cone increases, while the weak impact region first decreases and then increases, followed by the decreased temperature. On the contrary, the interference area expands with the decreased temperature. The outer region of the cone experiences atomization without significant changes in temperature. This phenomenon can be attributed to an even distribution of bottom surface temperatures at a nozzle tilt angle of 0°. The droplets are densely concentrated in the strong impact and interference areas with low temperatures. As the tilt angle escalates to 15°, an overlap occurs between the weak impact and interference regions, leading to a decline in temperature. However, droplet kinetic energy decreases due to nozzle interference from different directions, resulting in elevated temperatures within the strong impact zone. At a tilt angle of 30°, the kinetic energy of the droplets passing through the interference areas further decays, causing the droplets near the nozzle to almost vertically strike against the bottom surface. The interaction between these factors leads to an increase in the temperature distribution of the bottom surface within the interference regions. In the strong impact regions, the temperature outside these regions decreases.

Figure 12 shows the variation of the average heat transfer coefficient of the bottom surface at different tilt angles. The data indicates that as the tilt angle increases, the average heat transfer

coefficient for the two and four nozzles first decreases and then increases. For the three nozzles, it first increases slightly and then increases significantly. Compared with the two and four nozzles, the difference in behaviour of the three nozzles can be attributed to the changes in the spray coverage area. Specifically, as the tilt angle increases, this area first decreases before expanding again. However, due to their asymmetric arrangement, the three nozzles have an impact on coverage distribution and liquid film uniformity. When the inclination angle of all three nozzles reaches 15°, the interaction between these factors increases slightly in the heat transfer coefficient of the bottom surface.

The increase of the tilt angle can improve the heat transfer ability of the nozzle group. Optimizing the nozzle tilt angle (especially at 30°) can achieve a more uniform temperature distribution and significantly improve heat transfer efficiency. Table 2 shows the variations of nozzle group parameters under different tilt angles.

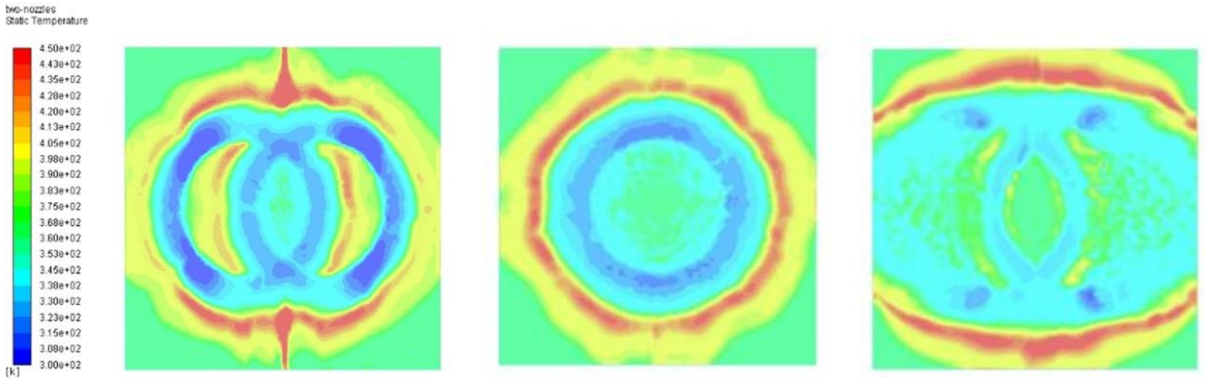

(a) 0° (b) 15° (c) 30°

Fig. 9. Temperature distribution on the bottom surface of two nozzles at different tilt angles.

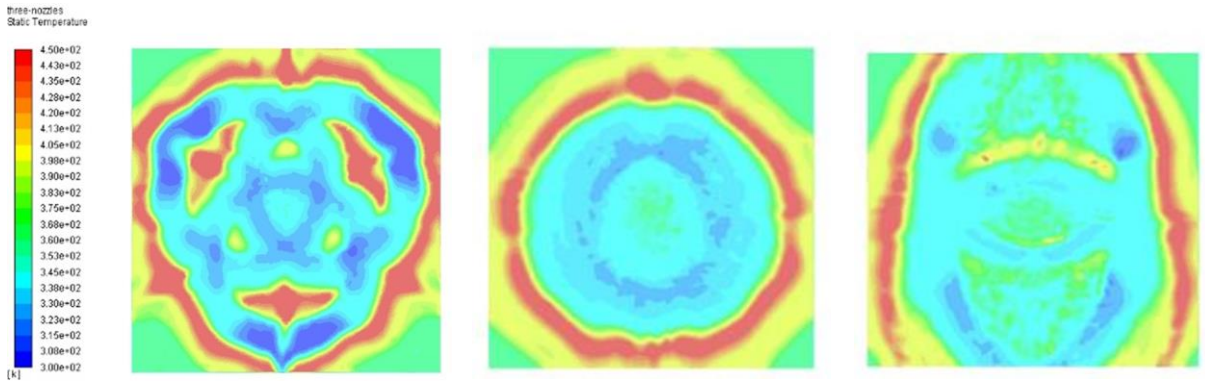

(a) 0° (b) 15° (c) 30°

Fig. 10. Temperature distribution on the bottom surface of three nozzles at different tilt angles.

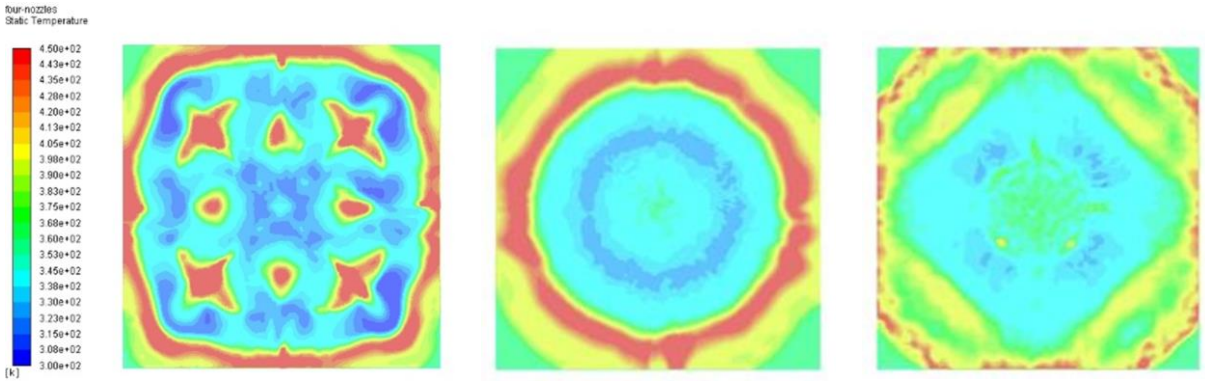

(a) 0° (b) 15° (c) 30°

Fig. 11. Temperature distribution on the bottom surface of four nozzles at different tilt angles.

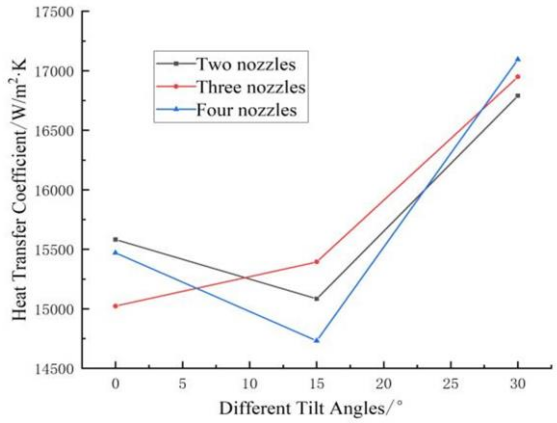

Fig. 12. Heat transfer coefficient curves at different tilt angles.

Table 2. Parameters of the nozzle group at different tilt angles.

Number of nozzles	Tilt angles, °	Average bottom surface temperature, K	Average liquid film temperature, K	Heat transfer coefficient, W/(m²·K)
Two	0	372.37	308.19	15582.54
	15	374.27	307.97	15084.03
	30	369.91	310.36	16790.07
Three	0	374.16	307.59	15023.26
	15	376.54	311.58	15393.46
	30	369.83	310.83	16948.77
Four	0	371.84	307.20	15469.86
	15	380.01	312.12	14731.37
	30	371.15	312.65	17095.22

3.3. Effect of nozzle group spacing

Figure 13 shows the variation of the average temperature on the bottom surfaces of the two, three and four nozzles with different nozzle group spacing. As the nozzle group spacing increases, the temperature of the three and four nozzles first increases and then decreases, while that of the two nozzles always shows a downward trend. This phenomenon can be attributed to significant interference effects between the three and four nozzles at a spacing of 2 mm. When this distance increases to 4 mm, although the coverage area of the spray is expanded, the interference effect will be weakened. Consequently, the average temperature on the bottom surface is observed to increase.

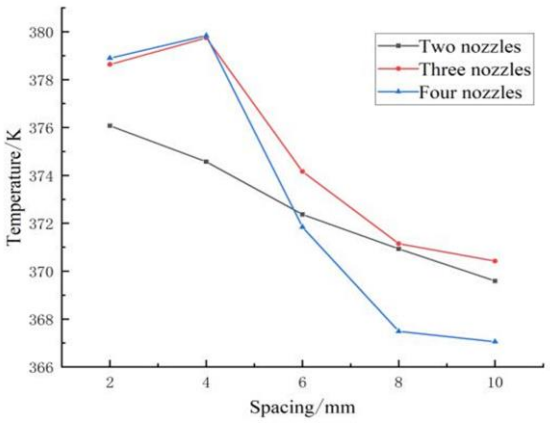

Fig. 13. Temperature curves at different nozzle distance.

Figures 14, 15, and 16 show the average temperature distribution on the bottom surface of configurations with two, three and four nozzles at different nozzle group spacing. At a nozzle spacing of 2 mm, there will be obvious interference between nozzles, resulting in overlapping of spray coverage areas and lower temperatures in the droplet impact zones. As the spacing between nozzles increases by 6 mm, this interference decreases. Consequently, the spray coverage area expands outward, causing a decreased temperature in the regions of strong impact while the temperature in the weak impact regions increases. In addition, the high-temperature region outside the atomization cone transitions from a continuous to discontinuous pattern. When the nozzle group spacing increases to 10 mm, the spray coverage area continuously expands, while the interference region decreases. The overall temperature is also decreasing. Specifically, the temperature in the weak hitting area of the atomization cone decreases, while that in strong hitting areas increases. High-temperature regions outside the atomization cone are concentrated at the upper and lower ends of this area, resulting in a more uniform temperature distribution.

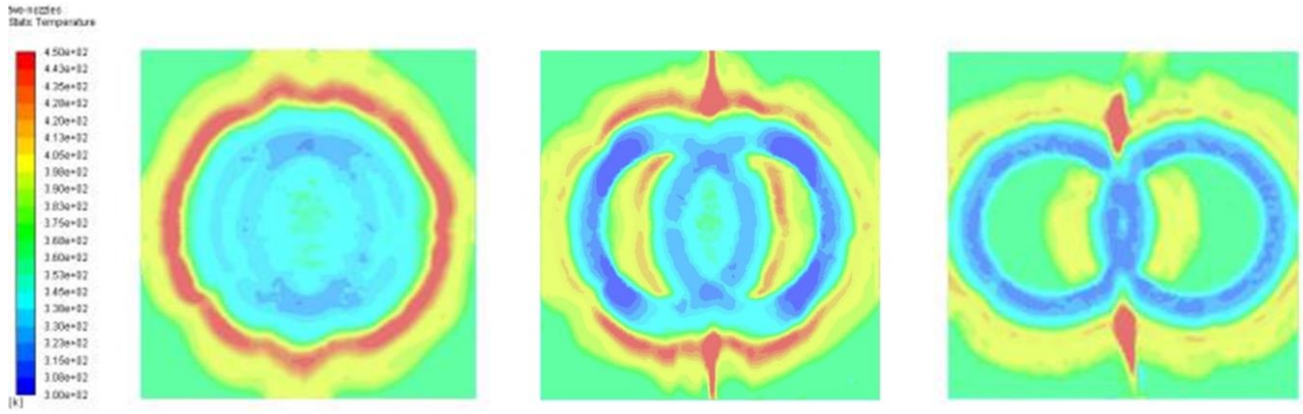

(a) 2 mm (b) 6 mm (c) 10 mm

Fig. 14. Temperature distribution on the bottom surface of two nozzles at different spacing.

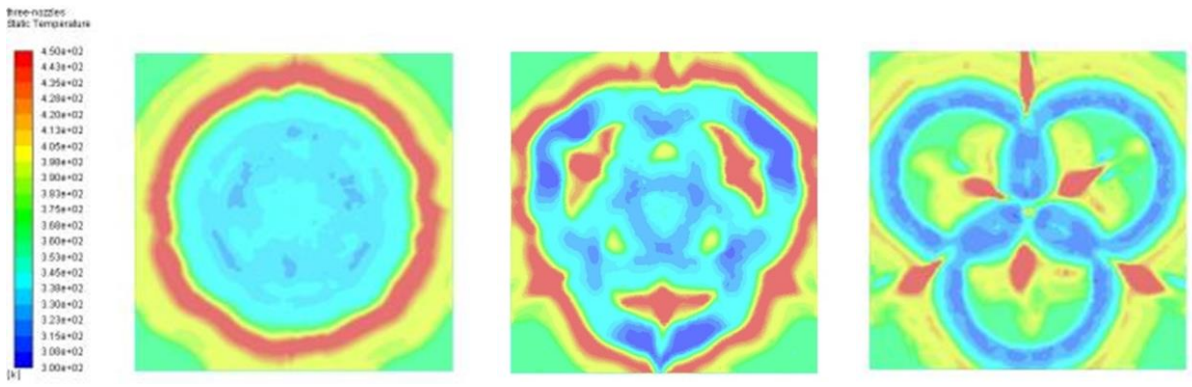

(a) 2 mm (b) 6 mm (c) 10 mm

Fig. 15. Temperature distribution on the bottom surface of three nozzles at different spacing.

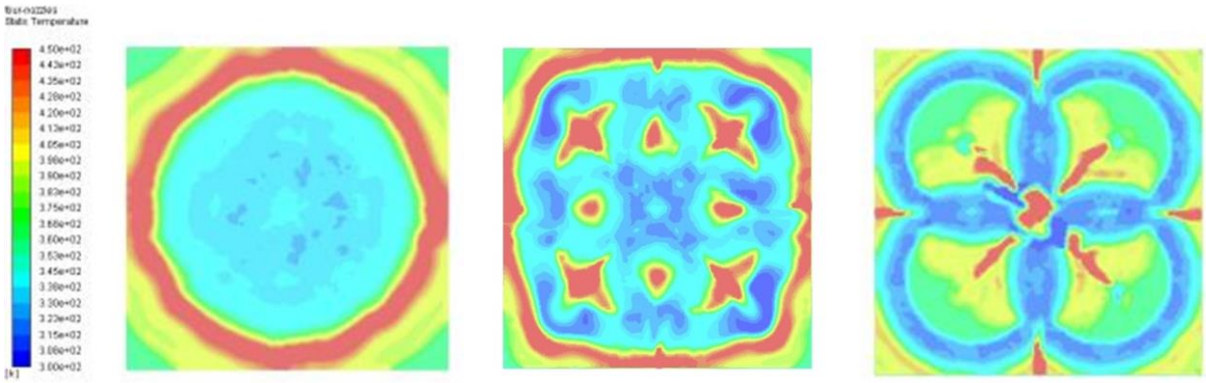

(a) 2 mm (b) 6 mm (c) 10 mm

Fig. 16. Temperature distribution on the bottom surface of four nozzles at different spacing.

As shown in Fig. 17, for two nozzles, the heat transfer coefficient of the bottom surface increases with the nozzle group spacing. In contrast, for three and four nozzles, a decrease is observed at a spacing of 6 mm, followed by a significant increase as the spacing continues to expand. This phenomenon can be attributed to the reduction of interference between nozzles when the spacing reaches 6 mm, which results in a dispersion of the droplet impact area.

However, it is worth noting that although the spray impact area does not fully cover the thermal wall and some liquid film overflows from its boundary, effective heat transfer would still occur at this stage. The temperature on the bottom surface decreases, and the average heat transfer coefficient also decreases. It is worth noting that during the temperature atomization cooling processes, the heat transfer coefficient of the bottom surface exceeds 14 750 W/(m^2·K).

Increasing the nozzle spacing within a specified range can significantly enhance the atomization cooling effect through improving droplet coverage and reducing interference zones, thereby enhancing heat transfer area and efficiency. Table 3 shows the variations of nozzle array parameters at different nozzle spacing.

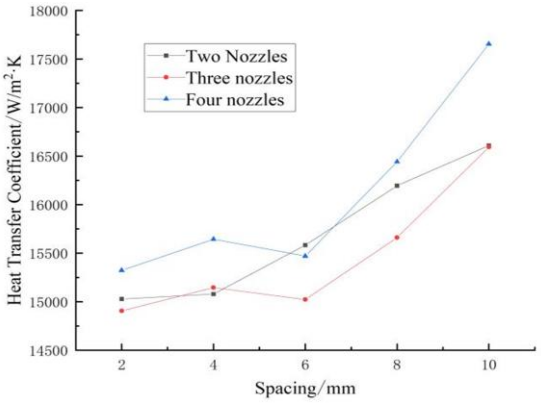

Fig. 17. Heat coefficient curves at different nozzle spacing.

Table 3. Parameters of the nozzle group at different nozzle spacing.

Number of nozzles	Spacing, mm	Average bottom surface temperature, K	Average liquid film temperature, K	Heat transfer coefficient, W/(m^2·K)
Two	2	376.07	309.53	15027.56
	6	372.37	308.19	15582.54
	10	369.59	309.38	16608.27
Three	2	378.63	311.54	14904,62
	6	374.16	307.59	15023.26
	10	370.42	310.15	16593.26
Four	2	378.90	313.63	15322.48
	6	371.84	307.20	15469.86
	10	367.05	310.40	17653.33

This study demonstrates that nozzle pressure, tilt angle and spacing have a significant impact on atomization cooling efficiency. External factors such as ambient temperature and fluid properties should not be ignored. Changes in ambient temperature can affect the evaporation rates of droplets and alter heat transfer efficiency. Moreover, the viscosity and density of different liquids will directly affect droplet size and velocity distribution, which in turn impacts cooling performance. In practical applications, these parameters should be adjusted according to specific operating conditions to optimize the cooling efficiency. Future research should further investigate the influence of these variables to improve the universality and practicality of the model.

4. Conclusions

This study analyses the effects of different pressures, tilt angles and spacing on the bottom temperature, liquid film temperature, liquid film thickness and heat transfer coefficient of the thermal wall of the nozzle array after atomization and cooling. The findings are drawn as follows:

(1) The increase in pressure can significantly improve the heat transfer capacity of the nozzle group. As the pressure increases, the thickness of the liquid film in the high-impact region of the atomization cone decreases. This leads to an increase in liquid film temperature, a reduction in bottom surface temperature, and an increase in heat transfer coefficient.

(2) The tilt angle of the nozzle significantly influences the heat transfer characteristics of the nozzle group. When the tilt angle reaches 30°, the average temperature of the bottom surface decreases, enabling the optimal heat transfer performance of the nozzle group. Under this configuration, a peak average heat transfer coefficient is observed. In addition, the bottom temperature distribution has good uniformity, and the liquid film is elliptical and can effectively reduce the retention areas. Conversely, at a tilt angle of 15°, the heat transfer efficiency of the nozzle group significantly decreases. Although the average temperature within the weak impact area of the atomization cone decreases, this will lead to an increase in the average temperature of the bottom surface and poor atomization cooling effects.

(3) The increase in nozzle spacing can increase the spray coverage area and improve the uniformity of temperature distribution in the nozzle array. When the distance between nozzles is set to 10mm within the range of 2 mm to 10 mm, the heat transfer performance is optimal. However, for the arrays with a limited number of nozzles, increasing the spacing may reduce the interaction between nozzles, which may lead to a decrease in overall heat transfer efficiency.

(4) Increasing the number of nozzles can improve the cooling efficiency of the nozzle array in a certain range. However, this enhancement is limited. In practical applications, economic factors such as costs related to nozzle manufacturing should be taken into account.

The relative impact on the heat transfer efficiency of the nozzle group ranks as: pressure > tilt angle > spacing > number of nozzles. When the nozzle group pressure is 2.0 MPa, the tilt angle is 30°, the nozzle spacing is 10 mm and the number of nozzles is 4, the heat transfer performance of the nozzle group is optimal. The numerical model has provided significant insights for optimizing atomization cooling parameters, and future work should combine experiments to validate these findings. An experimental study conducted under controlled conditions similar to those modelled in this study is crucial for verifying the accuracy and applicability of our results. This experimental validation may involve testing various nozzle configurations, pressures, tilt angles and spacing in real-world environments to ensure the robustness and reliability of our proposed guidelines.

Acknowledgements

This study was supported by the Applied Innovation Project of Hebei Vocational University of Technology and Engineering (No. 202307).

References

[1] Khandekar, S., Jaiswal, A.K., & Sahu, G. (2022). Spray cooling: From droplet dynamics to system level perspectives. *Advances in Heat Transfer*, 54, 135–177. doi: 10.1016/bs.aiht.2022.07.002

[2] Li, W., Zheng, Y., Shao, H., Wang, X., Chen, X., & Gao, Y. (2024). Experimental and Numerical Simulation Studies on the Atomization Characteristics of the Internal Mixing Nozzle and Its Field Application. *Mining, Metallurgy & Exploration*, 41(2), 1099–1120. doi: 10.1007/s42461-024-00955-x

[3] Mertens, R.G., Chow, L., Sundaram, K.B., Cregger, R.B., Rini, D.P., Turek, L., & Saarloos, B.A. (2007). Spray cooling of IGBT devices. *Journal of Electronic Packaging*, 129(3), 316–323. doi: 10.1115/1.2753937ss

[4] Zhang, H., Li, Y., Mao, Y., Tian, S., Liu, Y., & Yang, L. (2015). Optimization Design of a Novel Closed-Loop Spray Cooling System. *2015 IEEE International Conference on Advanced Intelligent Mechatronics*, Busan, Korea (South), IEEE, 324–329. doi: 10.1109/AIM.2015.7222552

[5] Pang, L.P., Luo, K., Guo, Q., Li, S.X., & Yang, C. (2017). Numerical study of high-overload effect on liquid film of spray cooling. *Applied Thermal Engineering*, 127, 1015–1024. doi: 10.1016/j.applthermaleng.2017.07.209

[6] Zheng, D., & Wang, M. (2022). Measurement of spray droplet velocity and size distribution by a tapered optical fiber probe. *2022 IEEE International Instrumentation and Measurement Technology Conference*, Ottawa, ON, Canada, IEEE, 1–6. doi: 10.1109/I2MTC48687.2022.9806586

[7] Majhool, A.A.A.K., & Jasim, N.M. (2020). Prediction of the Initial Drop Size and Velocity Distribution in the Cold Cryogenic Spray. *International Journal of Heat and Technology*, 38(3), 629–640. doi: 10.18280/ijht.380307

[8] Pautsch, A.G., & Shedd, T.A. (2006). Adiabatic and Diabatic Measurements of the Liquid Film Thickness During Spray Cooling with FC-72. *International Journal of Heat and Mass Transfer*, 49(15–16), 2610–2618. doi: 10.1016/j.ijheatmasstransfer.2006.01.024

[9] Selvam, R.P., Hamilton, M., & Silk, E.A. (2007). Spray cooling modeling: liquid film thickness effect on heat transfer. *AIP Conference Proceedings*, 880(1), 110–117. doi: 10.1063/1.2437447

[10] Liu, L., Wang, X., Ge, M., & Zhao, Y. (2021). Experimental study on heat transfer and power consumption of low-pressure

spray cooling. *Applied Thermal Engineering*, 184, 116253. doi: 10.1016/j.applthermaleng.2020.116253

[11] Li, J.X., Li, Y.Z., Li, E.H., & Li, T. (2020). Numerical Investigation on the Thermodynamic Characteristics of a Liquid Film upon Spray Cooling Using an Air-Blast Atomization Nozzle. *Entropy*, 22(3), 308. doi: 10.3390/e22030308

[12] Zhang, Z., Hu, D., Li, Q., Liu, C., & Zhou, F. (2021). Visualization study on atomization characteristics and heat transfer performance of R1336mzz flash spray cooling. *Science China Technological Sciences*, 64(10), 2099–2109. doi: 10.1007/ s11431-021-1853-4

[13] Hsieh, S.S., & Tsai, H.H. (2006). Thermal and flow measurements of continuous cryogenic spray cooling. *Archives of Dermatological Research*, 298(2), 82–95. doi: 10.1007/ s00403-006-0663-3

[14] Sapit, A., Razali, M.A., Mohammed, A.N., Manshoor, B., Khalid, A., Salleh, H., & Hushim, M.F. (2019). Study on Mist Nozzle Spray Characteristics for Cooling Application. *International Journal of Integrated Engineering*, 11(3), 299–303. doi: 10.30880/ijie.2019.11.03.033

[15] Durmuş, A., Durmuş, A., & Esen, M. (2002). Investigation of heat transfer and pressure drop in a concentric heat exchanger with snail entrance. *Applied Thermal Engineering*, 22(3), 321–332. doi: 10.1016/S1359-4311(01)00078-3

[16] Abbasi, B., & Kim, J. (2011). Development of a General Dynamic Pressure Based Single-Phase Spray Cooling Heat Transfer Correlation. *ASME Journal of Heat and Mass Transfer*, 133(5), 052201. doi: 10.1115/1.4002779

[17] Oflaz, F., Keklikcioglu, O., & Ozceyhan, V. (2022). Investigating thermal performance of combined use of SiO_2-water nanofluid and newly designed conical wire inserts. *Case Studies in Thermal Engineering*, 38, 102378. doi: 10.1016/j.csite.2022.102378

[18] Cheng, W.L., Liu, Q.N., Zhao, R., & Fan, H.L. (2010). Experimental Investigation of Parameters Effect on Heat Transfer of Spray Cooling. *Heat and Mass Transfer*, 46(8–9), 911–921. doi: 10.1007/s00231-010-0631-5

[19] Wang, Y., Liu, M., & Liu, D. (2017). Theoretical and Experimental Investigation of Heat Transfer Performance of Spray Cooling Under Low Mass Flux. *Journal of Engineering Thermophysics*, 31(6), 1027–1030. doi: 10.1007/s11630-017-1015-4

[20] Hou, Y. (2019). The Experimental Study and Numerical Simulation of Multi-Nozzle Spray Cooling. *Journal of Engineering Thermophysics*, 40(4), 678–683. doi: 10.1007/s11630-019-1127-7

[21] Muthukrishnan, S., Tan, X., & Srinivasan, V. (2023). High-efficiency spray cooling of rough surfaces with gas-assist atomization. *Applied Thermal Engineering*, 221, 119764. doi: 10.1016/ j.applthermaleng.2022.119764

[22] Liao, Y., Sakman, A.T., Jeng, S.M., Jog, M.A., & Benjamin, M.A. (1999). A Comprehensive Model to Predict Simplex Atomizer Performance. *Journal of Engineering for Gas Turbines and Power*, 121(2), 285–294. doi: 10.1115/1.2817119

[23] Si, C., Shao, S., & Tian, C. (2018). Experimental Study on Integrated Refrigeration-Spray Cooling System for High-Power Solid-State Laser. *Chinese Journal of Lasers*, 38(1), 44–48. doi: 10.3788/CJL20113801.0102008